Immunity, Volume *39*

Supplemental Information

Neonatal Fc Receptor Expression in Dendritic Cells Mediates Protective Immunity against Colorectal Cancer

Kristi Baker, Timo Rath, Magdalena B. Flak, Janelle C. Arthur, Zhangguo Chen, Jonathan N. Glickman, Inti Zlobec, Eva Karamitopoulou, Matthew D. Stachler, Robert D. Odze, Wayne I. Lencer, Christian Jobin, and Richard S. Blumberg

Supplemental Inventory

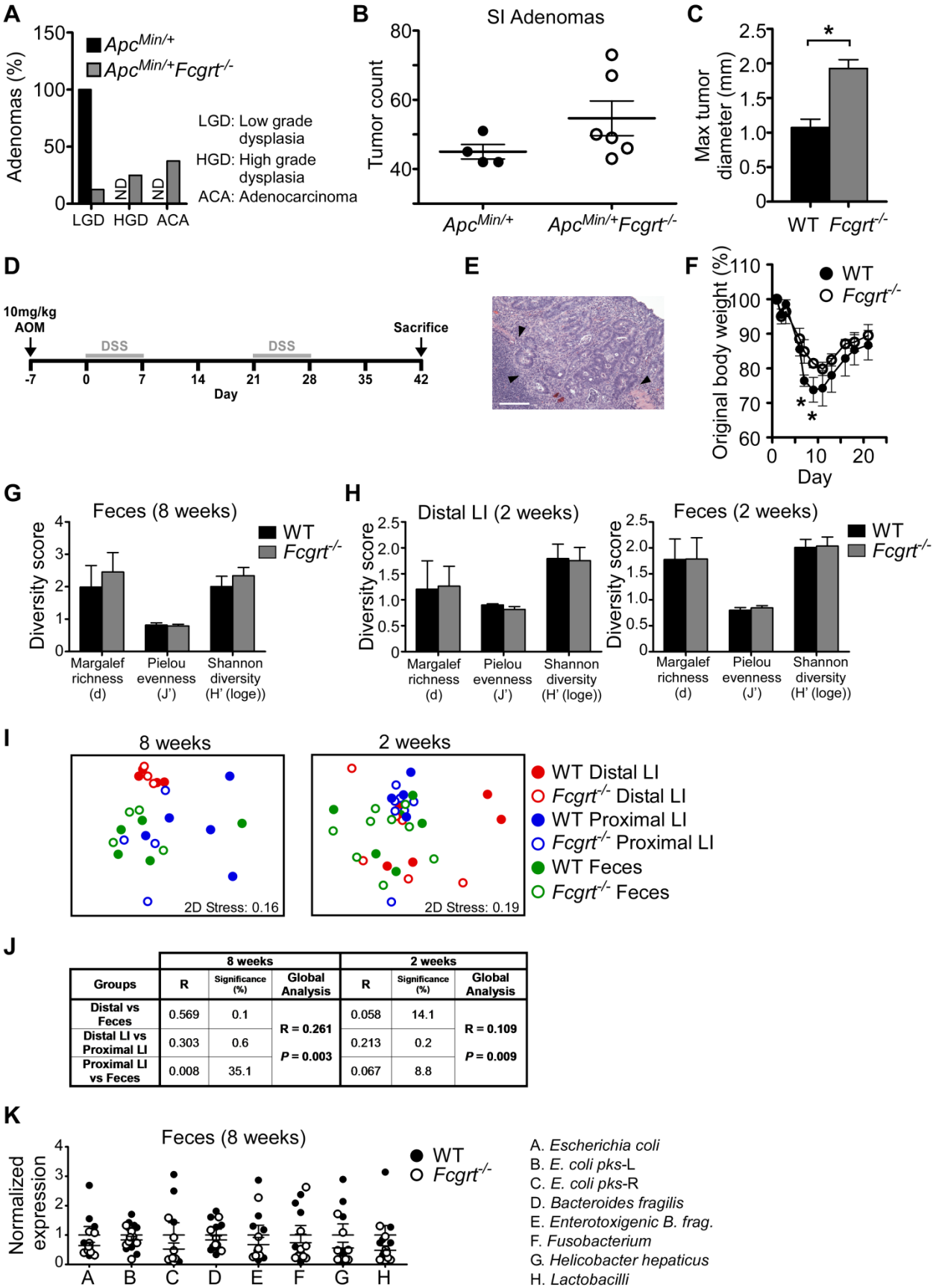

Groups	8 weeks R	8 weeks Significance (%)	8 weeks Global Analysis	2 weeks R	2 weeks Significance (%)	2 weeks Global Analysis
Distal vs Feces	0.569	0.1	R = 0.261	0.058	14.1	R = 0.109
Distal LI vs Proximal LI	0.303	0.6	P = 0.003	0.213	0.2	P = 0.009
Proximal LI vs Feces	0.008	35.1		0.067	8.8	

Figure S1. Loss of FcRn predisposes to the development of more severe inflammation- and non-inflammation-associated colorectal cancer (CRC) via a mechanism that is independent of intestinal microbiota. (A) Histological classification of adenomas present in the large intestine (LI) of *Apc*$^{Min/+}$ and *Apc*$^{Min/+}$*Fcgrt*$^{-/-}$ mice assessed at 5 months of age. (B) Frequency of adenomas in the small intestine (SI) of *Apc*$^{Mn/+}$ and *Apc*$^{Mn/+}$*Fcgrt*$^{-/-}$ mice. *n* = 4-6 mice per group in each of two independent experiments. (C) Maximum tumor diameter measured in WT and *Fcgrt*$^{-/-}$ mice treated with eight weekly doses of azoxymethane (AOM) in one representative experiment with *n* ≥ 3 mice per group. (D) Details of the azoxymethane/dextran sodium sulfate (AOM/DSS) treatment used for the induction of inflammation-associated colorectal cancer. Mice were treated with a single 10 mg/kg dose of AOM via i.p. injection (Day -7). Seven days later (Day 0), mice were given 1.5% DSS in their drinking water for a period of seven days. DSS was withdrawn and mice were allowed to drink regular water for 14 days (Day 7-21). The cycle of one week on DSS (Day 21-28) and two weeks on regular water (Day 28-42) was repeated once. Mice were sacrificed on Day 42. (E) Representative histology of the tumors present in both WT and *Fcgrt*$^{-/-}$ mice showing severe dysplasia and invasion (arrows) through the lamina propria in a lesion from an *Fcgrt*$^{-/-}$ mouse. Scale bar = 100 µm. (F) Weight curves during the first 20 days of treatment of mice undergoing AOM/DSS regimen. Mice were weighed every 1-2 days. Data are representative of two independent experiments with *n* = 5 mice per group per experiment. (G) Richness indices of microbiota found in the feces of untreated 8-week old WT and *Fcgrt*$^{-/-}$ littermates, as revealed by T-RFLP analysis. *n* = 3-5 mice per group. (H) Richness indices of microbiota found associated with the distal LI or feces of untreated 2-week old WT and *Fcgrt*$^{-/-}$ littermates, as revealed by T-RFLP analysis. *n* = 4-9 mice per group. (I) Multidimensional scaling (MDS) plots demonstrating microbial community composition in each of the indicated tissue compartments of untreated 8-week old and 2-week old WT and *Fcgrt*$^{-/-}$ mice as assessed by T-RFLP. ANOSIM analysis of Bray Curtis similarity matrices revealed no significant differences between WT and *Fcgrt*$^{-/-}$ mice for any age or tissue compartment. (J) ANOSIM results for analysis of microbial differences between tissue compartments within each age group, regardless of genotype. (K) Abundance of specific microbial species associated with the feces of untreated 7-week old WT and *Fcgrt*$^{-/-}$ mice as assessed by qPCR. Values from each species have been normalized to total bacteria (16S). Each dot represents an individual animal. *n* = 9 mice per group. All data represent mean ± s.e.m. ND = none detected. * $p \leq 0.05$. Figure S1, related to Figure 1.

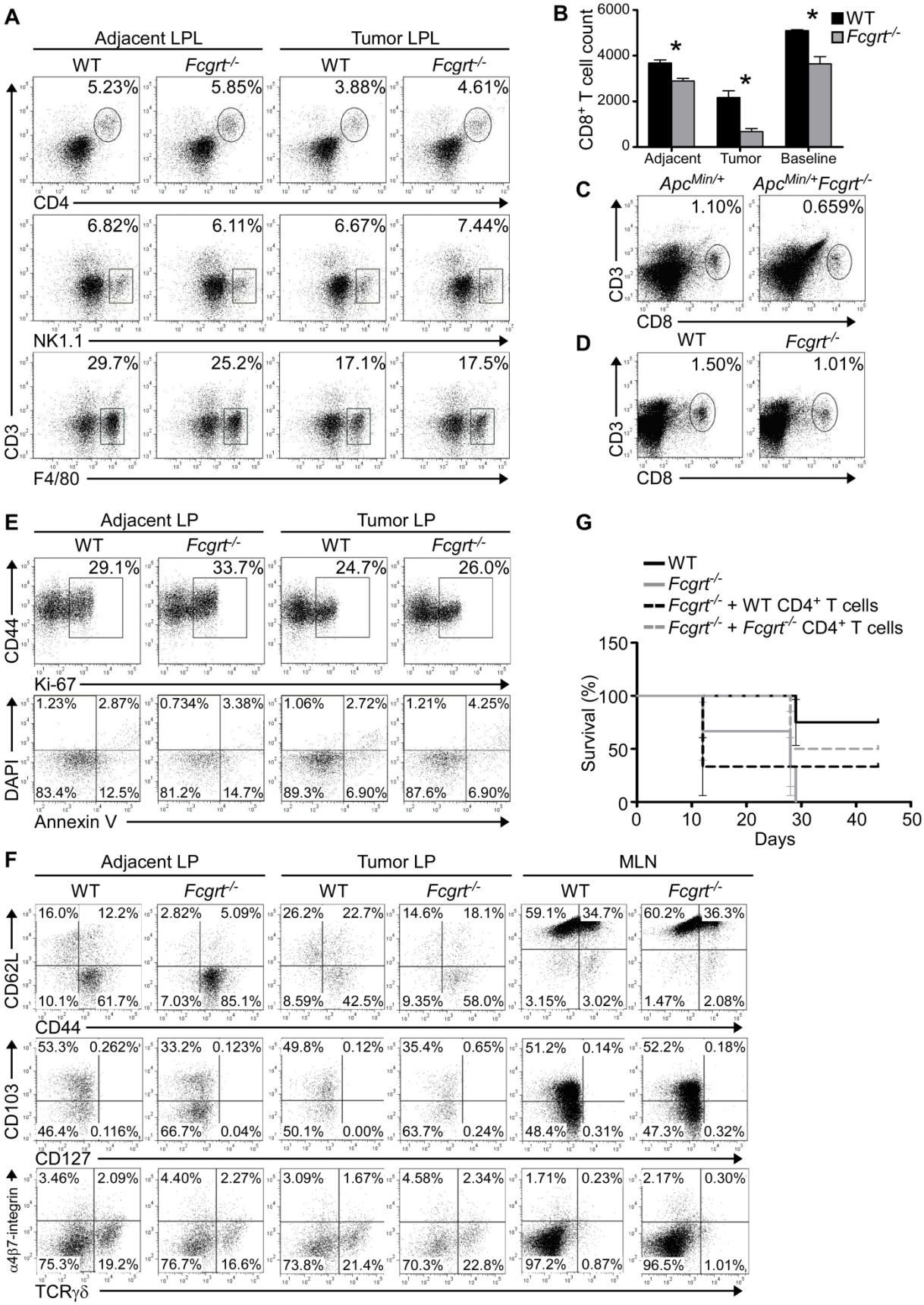
A
Adjacent LPL
Tumor LPL
WT
Fcgrt-/-
5.23%
5.85%
3.88%
4.61%
CD4
6.82%
6.11%
6.67%
7.44%
NK1.1
29.7%
25.2%
17.1%
17.5%
CD3
F4/80
B
CD8+ T cell count
6000
4000
2000
0
Adjacent
Tumor
Baseline
WT
Fcgrt-/-
C
ApcMin/+
ApcMin/+Fcgrt-/-
1.10%
0.659%
CD3
CD8
D
WT
Fcgrt-/-
1.50%
1.01%
CD3
CD8
E
Adjacent LP
Tumor LP
WT
Fcgrt-/-
29.1%
33.7%
24.7%
26.0%
CD44
Ki-67
1.23%
2.87%
0.734%
3.38%
1.06%
2.72%
1.21%
4.25%
83.4%
12.5%
81.2%
14.7%
89.3%
6.90%
87.6%
6.90%
DAPI
Annexin V
G
WT
Fcgrt-/-
Fcgrt-/- + WT CD4+ T cells
Fcgrt-/- + Fcgrt-/- CD4+ T cells
Survival (%)
150
100
50
0
0
10
20
30
40
50
Days
F
Adjacent LP
Tumor LP
MLN
WT
Fcgrt-/-
16.0%
12.2%
2.82%
5.09%
26.2%
22.7%
14.6%
18.1%
59.1%
34.7%
60.2%
36.3%
10.1%
61.7%
7.03%
85.1%
8.59%
42.5%
9.35%
58.0%
3.15%
3.02%
1.47%
2.08%
CD62L
CD44
53.3%
0.262%
33.2%
0.123%
49.8%
0.12%
35.4%
0.65%
51.2%
0.14%
52.2%
0.18%
46.4%
0.116%
66.7%
0.04%
50.1%
0.00%
63.7%
0.24%
48.4%
0.31%
47.3%
0.32%
CD103
CD127
3.46%
2.09%
4.40%
2.27%
3.09%
1.67%
4.58%
2.34%
1.71%
0.23%
2.17%
0.30%
75.3%
19.2%
76.7%
16.6%
73.8%
21.4%
70.3%
22.8%
97.2%
0.87%
96.5%
1.01%
α4β7-integrin
TCRγδ

Figure S2. FcRn-mediated tumor immune surveillance is mediated by selective activation and retention of CD8$^+$ T cells in the intestinal LP. (A) Flow cytometric analysis of the frequency of CD4$^+$ T cells, NK cells (NK1.1) or macrophages (F4/80) in the lamina propria lymphocyte (LPL) fraction of tumor and adjacent LI tissue in WT and *Fcgrt*$^{-/-}$ mice following AOM/DSS treatment. (B) Absolute number of CD8$^+$ T cells isolated from the LP tissue of the adjacent, tumor or untreated (baseline) LI in AOM/DSS-treated mice as assessed by flow cytometric staining and acquisition of fixed volumes of sample. (C-D) Flow cytometric analysis of the frequency of CD8$^+$ T cells in the lamina propria (LP) fraction of tumor-adjacent LI tissue in untreated *Apc*$^{Min/+}$ and *Apc*$^{Min/+}$*Fcgrt*$^{-/-}$ mice (C) and in AOM-treated WT and *Fcgrt*$^{-/-}$ littermates (D). Representative results from one of three experiments with *n* = 3 mice per group per experiment. (E) Flow cytometric analysis of the extent of CD8$^+$ T cell proliferation (Ki-67) and apoptosis (Annexin V) in the LP fraction of tumor and adjacent LI tissue in WT and *Fcgrt*$^{-/-}$ littermates following AOM/DSS treatment. Plots depict cells within the CD3$^+$CD8$^+$ gate of cells. Representative plots from three independent experiments with *n* = 3 mice per group per experiment. (F) Phenotype of CD8$^+$ T cells in the indicated tissue compartment of WT and *Fcgrt*$^{-/-}$ littermates treated with AOM/DSS. Representative plots from three independent experiments with *n* = 3-4 mice per group per experiment. (G) Survival rates of AOM/DSS-treated recipient mice adoptively transferred with CD4$^+$ T cells taken from the MLN and LI LP of AOM/DSS-treated WT and *Fcgrt*$^{-/-}$ donors. Representative results from one of two independent experiments with *n* = 4 mice per group per experiment. Significance of survival curves was assessed by Logrank test. All data represent mean ± s.e.m. * $p \leq 0.05$. Figure S2, related to Figure 2.

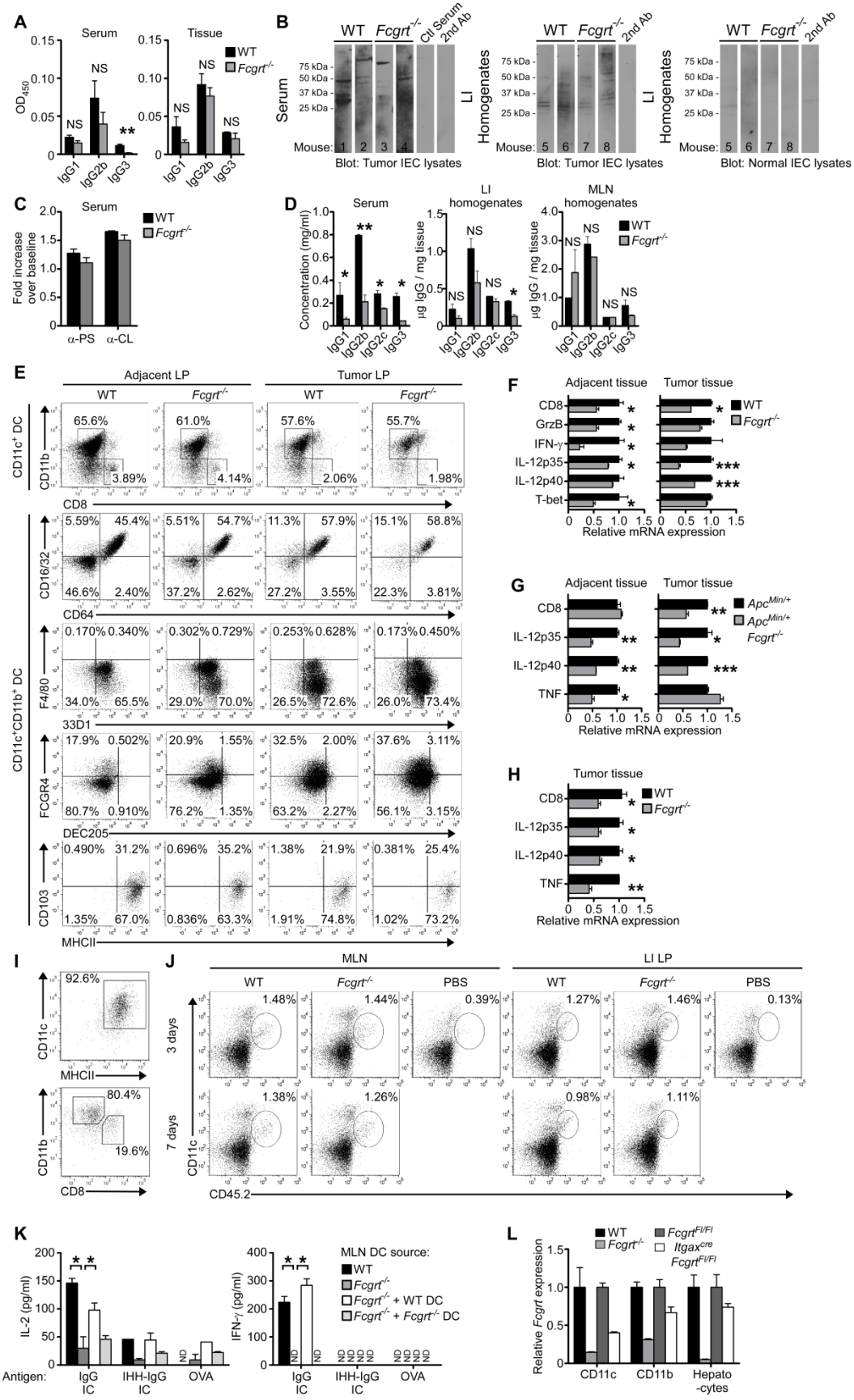
A
Serum
Tissue
WT
Fcgrt-/-
OD450
NS
**
IgG1
IgG2b
IgG3
B
WT
Fcgrt-/-
Ctl Serum
2nd Ab
Serum
LI Homogenates
75 kDa
50 kDa
37 kDa
25 kDa
Mouse: 1 2 3 4
Blot: Tumor IEC lysates
Mouse: 5 6 7 8
Blot: Tumor IEC lysates
Blot: Normal IEC lysates
C
Serum
Fold increase over baseline
α-PS
α-CL
D
Serum
LI homogenates
MLN homogenates
Concentration (mg/ml)
µg IgG / mg tissue
IgG1
IgG2b
IgG2c
IgG3
E
Adjacent LP
Tumor LP
CD11c+ DC
CD11b
CD8
65.6%
3.89%
61.0%
4.14%
57.6%
2.06%
55.7%
1.98%
CD16/32
CD64
5.59%
45.4%
46.6%
2.40%
5.51%
54.7%
37.2%
2.62%
11.3%
57.9%
27.2%
3.55%
15.1%
58.8%
22.3%
3.81%
CD11c+CD11b+ DC
F4/80
33D1
0.170%
0.340%
34.0%
65.5%
0.302%
0.729%
29.0%
70.0%
0.253%
0.628%
26.5%
72.6%
0.173%
0.450%
26.0%
73.4%
FCGR4
DEC205
17.9%
0.502%
80.7%
0.910%
20.9%
1.55%
76.2%
1.35%
32.5%
2.00%
63.2%
2.27%
37.6%
3.11%
56.1%
3.15%
CD103
MHCII
0.490%
31.2%
1.35%
67.0%
0.696%
35.2%
0.836%
63.3%
1.38%
21.9%
1.91%
74.8%
0.381%
25.4%
1.02%
73.2%
F
Adjacent tissue
Tumor tissue
CD8
GrzB
IFN-γ
IL-12p35
IL-12p40
T-bet
Relative mRNA expression
G
Adjacent tissue
Tumor tissue
ApcMin/+
ApcMin/+ Fcgrt-/-
CD8
IL-12p35
IL-12p40
TNF
Relative mRNA expression
H
Tumor tissue
CD8
IL-12p35
IL-12p40
TNF
Relative mRNA expression
I
92.6%
CD11c
MHCII
80.4%
19.6%
CD11b
CD8
J
MLN
LI LP
WT
Fcgrt-/-
PBS
3 days
7 days
CD11c
CD45.2
1.48%
1.44%
0.39%
1.27%
1.46%
0.13%
1.38%
1.26%
0.98%
1.11%
K
IL-2 (pg/ml)
IFN-γ (pg/ml)
MLN DC source:
WT
Fcgrt-/-
Fcgrt-/- + WT DC
Fcgrt-/- + Fcgrt-/- DC
Antigen:
IgG IC
IHH-IgG IC
OVA
ND
L
WT
Fcgrt-/-
FcgrtFl/Fl
Itgaxcre FcgrtFl/Fl
Relative Fcgrt expression
CD11c
CD11b
Hepato-cytes

Figure S3. **FcRn-dependent dendritic cell (DC)-mediated tumor protection is associated with the presence of tumor-antigen reactive IgG in intestinal tissues and the generation of a local Th1/Tc1 polarizing cytokine environment.** (A) Isotype distribution of tumor antigen-specific IgG in the serum or LI homogenates of AOM/DSS treated WT or *Fcgrt*$^{-/-}$ mice. ELISA plates coated with lysates from tumor epithelium were probed with dilutions of serum or tissue homogenates from tumor bearing mice and developed with isotype-specific secondary antibodies. (B) Immunoblots demonstrating tumor antigen-specific IgG in the serum and LI homogenates of each of eight AOM/DSS treated mice. IgG-depleted lysates prepared from tumor intestinal epithelial cells (IEC) or non-tumor control IEC were resolved under reducing conditions by SDS-PAGE and membranes of the transferred lysates were probed with serum or LI homogenates from tumor bearing mice. Representative blots from two independent experiments with n = 4 mice per group per experiment. 2nd Ab = anti-mouse IgG-HRP. (C) Fold increase above baseline values in serum anti-phosphatidylserine (α-PS) and anti-cardiolipin (α-CL) IgG content in WT and *Fcgrt*$^{-/-}$ littermates. (D) IgG isotype content of the serum, LI homogenates and MLN homogenates in AOM/DSS-treated WT and *Fcgrt*$^{-/-}$ mice. (E) Flow cytometric analysis of the frequency of CD8^{+} versus CD11b^{+} DC (top row, gated on CD11c^{+} cells) and characterization of the CD11c^{+}CD8^{-}CD11b^{+} DC (bottom four rows) in the mucosal tissues of AOM/DSS-treated WT and *Fcgrt*$^{-/-}$ littermates. (F-H) Whole tissue cytokine transcript profiles of the indicated tissue compartments from AOM/DSS-treated WT and *Fcgrt*$^{-/-}$ littermates (F), untreated *Apc*$^{Min/+}$ and *Apc*$^{Min/+}$*Fcgrt*$^{-/-}$ littermates (G) and AOM-treated WT and *Fcgrt*$^{-/-}$ littermates (H). Representative results from 2-4 independent experiments with n = 3-6 mice per group per experiment. Data represent mean ± s.e.m. (I) Purity (top panel) and subset distribution (bottom panel) of the DC transferred in Figure 3C,F. (J) Frequency of congenic (CD45.2) WT or *Fcgrt*$^{-/-}$ DC in the MLN and LI LP of recipient (CD45.1) mice 3 days and 7 days after intraperitoneal transfer. Recipient mice injected with PBS are shown as controls. (K) *Ex vivo* antigen cross-presentation with DC isolated from the MLN of the indicated AOM/DSS-treated DC recipient mice and loaded with IC containing FcRn-binding (IgG) immune complex (IC), non-FcRn binding (IHH-IgG) IC or soluble antigen (OVA) and cocultured with OT-I CD8^{+} T cells. (L) Relative *Fcgrt* transcript levels as assessed by qPCR in DC (CD11c), macrophages (CD11b) and hepatocytes purified from WT, *Fcgrt*$^{-/-}$, *Fcgrt*$^{Fl/Fl}$ or *Itgax*^{cre}*Fcgrt*$^{Fl/Fl}$ mice. Data are representative of two independent experiments with n = 3-5 mice per group per experiment. All data represent mean ± s.e.m. * $p \leq 0.05$, ** $p \leq 0.01$, *** $p \leq 0.005$. Figure S3, related to Figure 3.

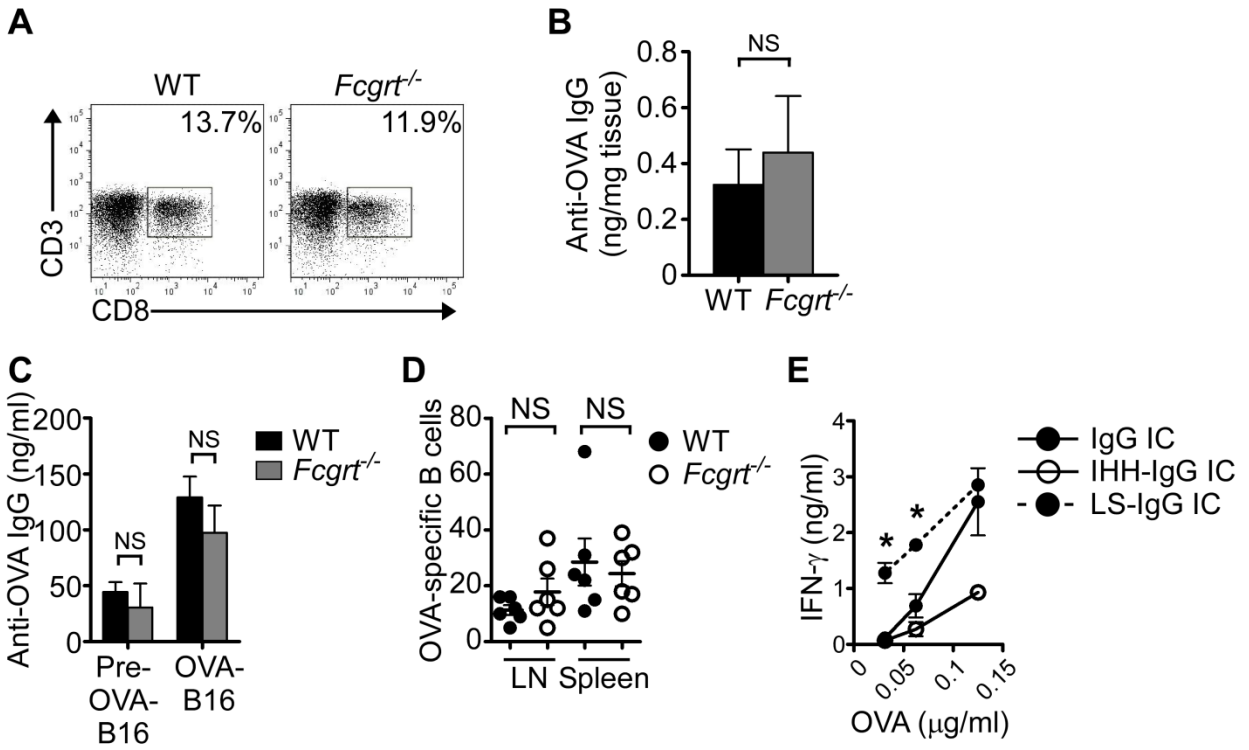

Figure S4. Both CD8$^+$ T cells and tumor-specific IgG are required for FcRn-mediated protection from pulmonary metastases. (A) CD8$^+$ T cell frequency in the lungs of untreated WT or *Fcgrt*$^{-/-}$ mice. (B-C) Tumor-specific anti-OVA IgG in the lung homogenates (B) or serum (C) of WT and *Fcgrt*$^{-/-}$ littermates bearing lung metastases. Lungs were harvested 2 weeks after i.v. injection of 0.5x10^6 OVA-expressing B16 melanoma cells (OVA-B16). Anti-OVA IgG content was evaluated by ELISA and normalized to protein content of the homogenates for (B). (D) Frequency of OVA-specific IgG producing B cells in the lymph nodes (LN) or spleens of OVA-B16 lung metastasis-bearing WT and *Fcgrt*$^{-/-}$ mice. B cells were isolated and cultured on OVA-coated ELISpot plates for 24 h. (E) *Ex vivo* antigen cross-presentation using DC stimulated with immune complexes (IC) formed with NIP-OVA and either FcRn-binding (IgG IC), non-FcRn binding (IHH-IgG IC) or enhanced FcRn-binding (LS-IgG IC) immunoglobulin and cocultured with OT-I CD8$^+$ T cells. All data are representative of the results of one of three independent experiments with n = 3-6 mice per group per experiment. Data represent mean ± s.e.m. NS = not significant. * $p \leq 0.05$. Figure S4, related to Figure 4.

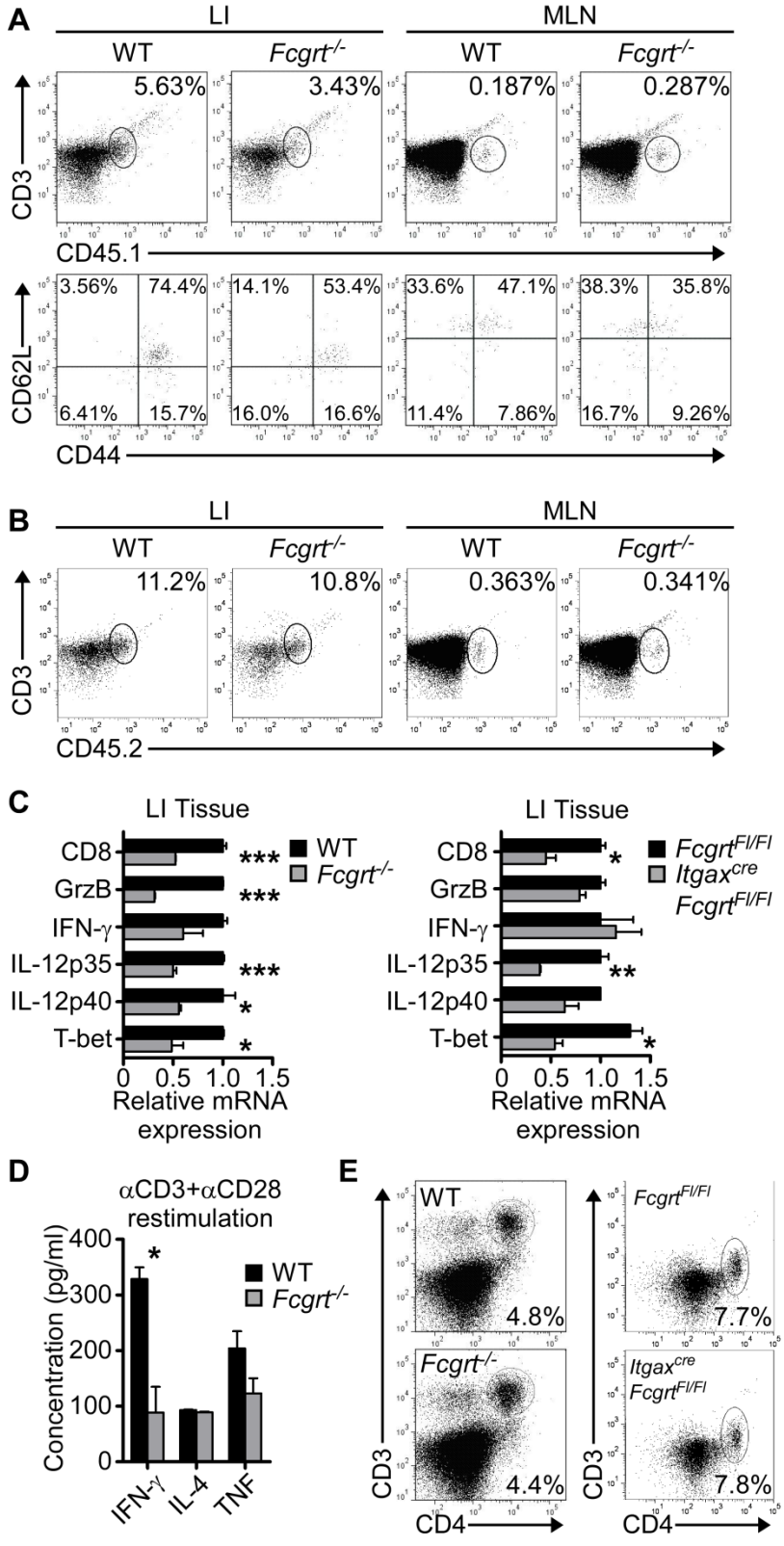
A
LI
MLN
WT
Fcgrt-/-
WT
Fcgrt-/-
5.63%
3.43%
0.187%
0.287%
CD3
CD45.1
3.56%
74.4%
14.1%
53.4%
33.6%
47.1%
38.3%
35.8%
6.41%
15.7%
16.0%
16.6%
11.4%
7.86%
16.7%
9.26%
CD62L
CD44
B
LI
MLN
WT
Fcgrt-/-
WT
Fcgrt-/-
11.2%
10.8%
0.363%
0.341%
CD3
CD45.2
C
LI Tissue
CD8
GrzB
IFN-γ
IL-12p35
IL-12p40
T-bet
***
***
***
*
*
WT
Fcgrt-/-
0 0.5 1.0 1.5
Relative mRNA expression
LI Tissue
CD8
GrzB
IFN-γ
IL-12p35
IL-12p40
T-bet
*
**
*
FcgrtFl/Fl
Itgaxcre FcgrtFl/Fl
0 0.5 1.0 1.5
Relative mRNA expression
D
αCD3+αCD28 restimulation
Concentration (pg/ml)
400
300
200
100
0
*
WT
Fcgrt-/-
IFN-γ
IL-4
TNF
E
WT
4.8%
Fcgrt-/-
4.4%
FcgrtFl/Fl
7.7%
Itgaxcre FcgrtFl/Fl
7.8%
CD3
CD4

Figure S5. FcRn in DC drives homeostatic local activation of $CD8^+$ T cells and the Th1 polarization of $CD4^+$ T cells within the LI LP by facilitating the production of Tc1 and Th1 polarizing cytokines. (A) Frequency (upper panels) and effector status (lower panels) of adoptively transferred congenic $CD8^+$ T cells (CD45.1) in the LI LP and MLN of untreated WT and *Fcgrt*$^{-/-}$ recipient mice (CD45.2). $1x10^6$ $CD8^+$ T cells were transferred into recipient mice via i.v. injection and their distribution and phenotype was assessed 10 days later. (B) Frequency of adoptively transferred congenic $CD8^+$ T cells from WT and *Fcgrt*$^{-/-}$ donor mice (CD45.2) in the LI LP and MLN of untreated recipient mice (CD45.1) 7 days after transfer. (C) Whole tissue transcript profiles of the LI from untreated WT and *Fcgrt*$^{-/-}$ littermates (left panel) or *Fcgrt*$^{Fl/Fl}$ and *Itgax*^{cre}*Fcgrt*$^{Fl/Fl}$ littermates (right panel), as assessed by qPCR. (D) Cytokine secretion by $CD4^+$ T cells isolated via magnetic sorting from the LI LP of untreated WT and *Fcgrt*$^{-/-}$ mice and restimulated for 24 h with anti-CD3 (αCD3) and anti-CD28 (αCD28). (E) $CD4^+$ T cell frequency in the LI LP of untreated WT and *Fcgrt*$^{-/-}$ mice (left panels) or *Fcgrt*$^{Fl/Fl}$ and *Itgax*^{cre}*Fcgrt*$^{Fl/Fl}$ mice (right panels). Representative results from three independent experiments with n = 3-5 mice per group per experiment. Data represent mean ± s.e.m. * $p \leq 0.05$, ** $p \leq 0.01$, *** $p \leq 0.005$. Figure S5, related to Figure 5.

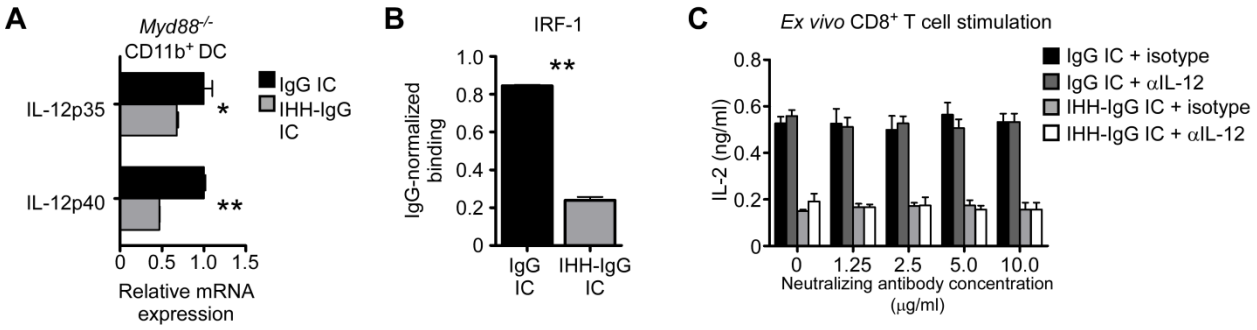

Figure S6. FcRn-dependent induction of IL-12 is not dependent on MYD88 and is not required for FcRn-mediated cross-priming. (A) Induction of IL-12p35 upon *ex vivo* stimulation of *Myd88*$^{-/-}$ CD8^{-}CD11b^{+} DC with FcRn-binding IC (IgG IC) or FcRn non-binding IC (IHH-IgG IC) for 6 h. (B) Binding of IRF-1 to the IL-12p35 promoter upon stimulation of *Myd88*$^{-/-}$ CD8^{-}CD11b^{+} DC with IgG IC or IHH-IgG IC for 4 h. (C) *Ex vivo* antigen cross-presentation in the presence of an IL-12 neutralizing antibody (αIL-12) or isotype control. DC were stimulated with IgG IC or IHH-IgG IC and co-cultured with OT-I CD8^{+} T cells. Representative data shown from one of three independent experiments. Data represent mean ± s.e.m. * $p \leq 0.05$, ** $p \leq 0.01$. Figure S6, related to Figure 6.

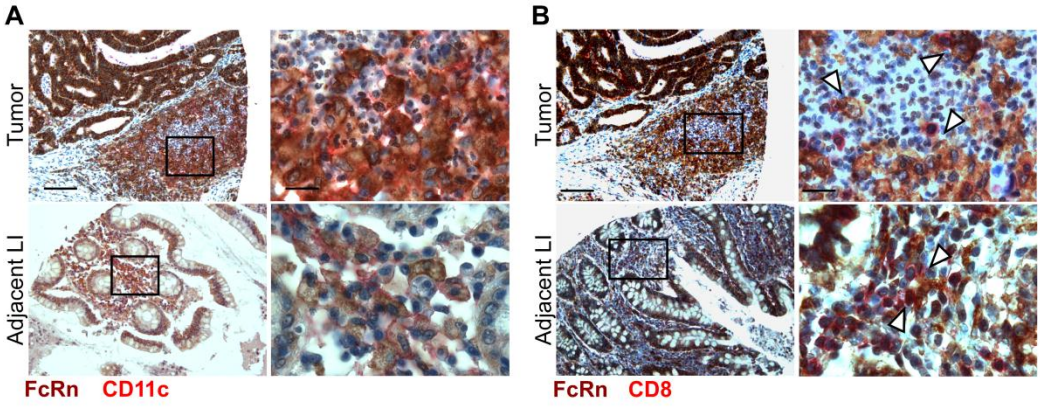

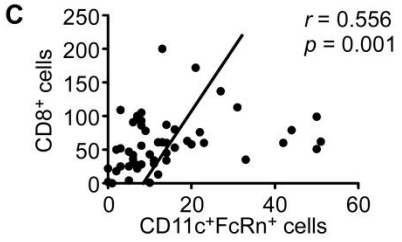

D

Feature	HR (95% CI)	p-value
CD11c+FcRn+	0.97 (0.94-0.99)	0.0388
pN classification	4.35 (2.07-9.12)	0.0001
pT classification	1.4 (0.58-3.38)	0.4504
pM classification	2.92 (1.49-5.72)	0.0018
Adjuvant therapy	0.65 (0.35-1.23)	0.1850

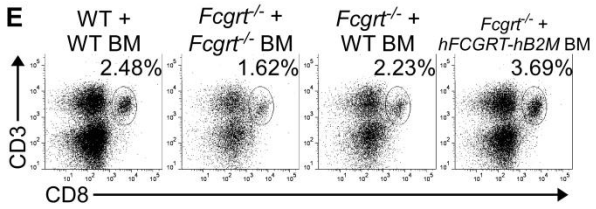

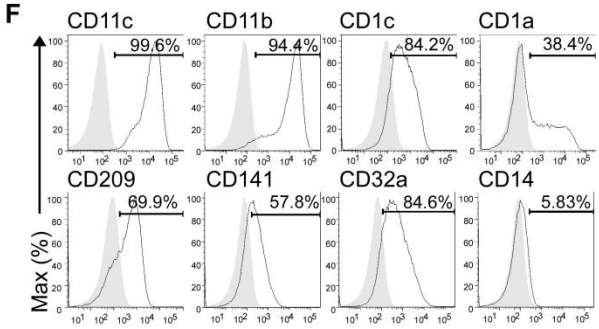

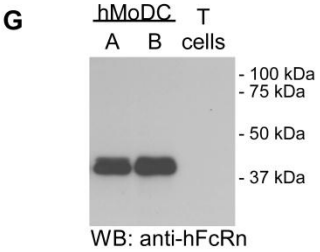

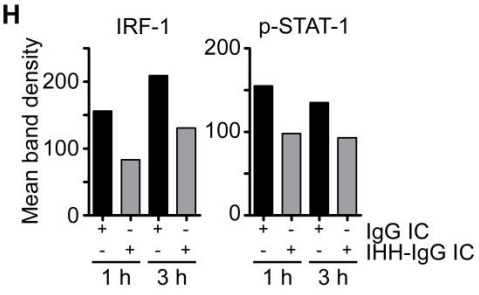

Figure S7. Human DC strongly express FcRn and localize to the stroma of both normal and CRC-associated LI. (A) Double immunohistochemical staining of $FcRn^+CD11c^+$ DC in the stroma of CRC-bearing (upper panels) and tumor-adjacent normal (lower panels) LI of additional cases of human CRC. FcRn = brown, CD11c = red. See also Figure 7A. Scale bar left panels = 100 μm. Scale bar right panels = 20 μm. (B) Colocalization of $FcRn^+$ DC (brown) and $CD8^+$ T cells (red) in the stroma of CRC-bearing (upper panels) and tumor-adjacent normal (lower panels) LI of additional cases of human CRC. Arrowheads indicate areas of colocalization. See also Figure 7B. Data in panels A-B are representative of 50 matched normal LI and CRC assessed. (C) Correlation between the number of $FcRn^+CD11c^+$ DC and $CD8^+$ T cells in the stroma of normal LI adjacent to CRC. Significance was assessed using Spearman's rank correlation. (D) Multivariable analysis of the impact of colonic LP $CD11c^+FcRn^+$ cells on patient survival in 183 human CRC patients. An increasing number of $CD11^+FcRn^+$ cells has a positive effect on patient survival (univariate analysis $p = 0.0333$) and this effect is maintained in multivariable analysis with the indicated parameters. See also Figure 7C. (E) $CD8^+$ T cell frequency in the tumor LP of chimeric mice treated with AOM/DSS. WT recipients were reconstituted with bone marrow from WT donors. *Fcgrt*$^{-/-}$ recipients were reconstituted with bone marrow from either *Fcgrt*$^{-/-}$, WT or *hFCGRT-hB2M-mFcgrt*$^{-/-}$ donors. Representative results from one of two independent experiments with $n = 4$-5 mice per group per experiment. (F) Phenotype of human monocyte derived DC (hMoDC) as determined by flow cytometric analysis. Shaded curve represents isotype control. (G) Expression of FcRn in hMoDC, as assessed by the same antibody utilized for immunohistochemical staining of CRC cases. (H) Densitometric analysis of Western blots of hMoDC stimulated with IgG IC depicted in Figure 7F. Data in panels F-H are representative of six donors processed in pairs in each of three independent experiments. All data represent mean ± s.e.m. Figure S7, related to Figure 7.

Supplemental Experimental Procedures

Mice. *Fcgrt*$^{-/-}$ mice (Roopenian et al., 2003), deficient in FcRn, on a C57BL/6 background were originally purchased from The Jackson Laboratory and maintained in our animal facility where they have been further backcrossed onto the C57BL/6 for a total of 21 generations. Both WT and *Fcgrt*$^{-/-}$ mice for all experiments were generated from the breeding of parents heterozygous for *Fcgrt* expression (ie. *Fcgrt*$^{+/-}$). Matched WT and *Fcgrt*$^{-/-}$ littermates were used in all experiments. *Fcgrt*$^{Fl/Fl}$ mice were a kind gift of Dr. E. Sally Ward (University of Texas Southwestern Medical Center) (Montoyo et al., 2009). *hFCGRT-hB2M-mFcgrt*$^{-/-}$ mice have been described previously (Montoyo et al., 2009; Yoshida et al., 2004). *Apc*$^{Min/+}$, *Myd88*$^{-/-}$, Ly5.1 and OT-I mice were purchased from The Jackson Laboratory. *Stat1*$^{-/-}$ mice were purchased from Taconic. All procedures were approved by the Harvard Medical Area Standing Committee on Animals.

Induction of colorectal cancer. Inflammation-associated CRC was induced by a single i.p. dose of 10 mg/kg azoxymethane (AOM) (Sigma Aldrich) and the subsequent administration of two 7-day courses of 1.5% dextran sodium sulfate (DSS) (MP Biomedicals) in drinking water, as outlined in Figure S1D and described previously (Wirtz et al., 2007). Tumor burden was assessed two weeks after withdrawal of the final course of DSS. Tumor load was calculated as the sum of all tumor diameters, as described previously (Grivennikov et al., 2012). Bone marrow chimeras were generated by lethal irradiation of recipients (2 x 6 Gy) followed by reconstitution with 1 x 10^6 bone marrow cells from the appropriate donor. Treatment of the chimeras with AOM/DSS was begun 8 weeks after reconstitution. Non-inflammation-associated CRC was induced by eight weekly i.p. injections of 10 mg/kg AOM. Tumor burden was assessed 12 weeks after administration of the final dose of AOM. Tumor burden in *Apc*$^{Min/+}$ and *Apc*$^{Min/+}$*Fcgrt*$^{-/-}$ mice was assessed at 5-6 months of age in untreated mice. In all experiments, tumor evaluation

was carried out blindly by counting macroscopically visible tumors (>1 mm in diameter) and measuring the largest diameter of each lesion with digital calipers.

Adoptive transfer experiments. $CD8^+$ T cells or DC from the MLN and LI lamina propria were isolated from donor mice at day 21 of the AOM/DSS treatment course (see Figure S1D). Isolation of cells was carried out by sequential collagenase digestions, as previously described (Baker et al., 2011). $CD8^+$ T cells were subsequently purified using negative magnetic selection (Miltenyi Biotec). DC were purified using positive magnetic selection with CD11c-microbeads (Miltenyi Biotec) and yielded predominantly $CD8^-CD11b^+$ DC **(**Figure S3I). $1x10^6$ $CD8^+$ T cells or DC were adoptively transferred to recipient mice via i.p. injection, on days 0 and 21 for $CD8^+$ T cells and days -7 and 14 for DC. Appropriate localization of the transferred cells to the MLN and LI lamina propria of the recipient mice was verified in separate experiments using mice congenic for Ly5.1 expression (Figure S3J). For depletion of $CD8^+$ T cells, mice were initially treated i.p. on consecutive days with three doses of 0.5 mg of an anti-CD8 antibody (clone 53-6.72, BWH-BRI Antibody Core Facility) (or isotype control) beginning 3 days prior to the initial DC transfer (Kruisbeek, 1991). Thereafter, $CD8^+$ T cell depletion was maintained by administration of 0.5 mg anti-CD8 antibody (or isotype) every three days until termination of the experiment. For IL-12 neutralization, mice were initially treated on consecutive days with three i.p. doses of 0.5 mg of an anti-IL-12p40 antibody (clone C17.8) (kindly provided by Dr. Giorgio Trinchieri, National Cancer Institute) (or isotype control) beginning 3 days prior to the initial DC transfer. Neutralization was maintained by administration of 0.5 mg anti-IL-12p40 antibody (or isotype) twice per week until termination of the experiment.

Lung metastasis experiments. Lung metastases were induced by the i.v. injection of $0.5x10^6$ OVA-transfected B16 melanoma cells (OVA-B16 cells, a generous gift of Dr. Kenneth Rock, University of Massachusetts Medical School) in log phase growth (Falo et al., 1995;

LeibundGut-Landmann et al., 2008). Evaluation of lung nodules was carried out following lung inflation and fixation in 10% formalin. For DC immunization experiments, DC were isolated by collagenase digestion from the lung and draining lymph nodes of metastasis-bearing donor mice and $1x10^6$ DC were injected s.c. into the hind footpad of recipient mice. Two weeks later, recipients were given OVA-B16 cells, as above. For $CD8^+$ T cell protection experiments, OVA-specific OT-I $CD8^+$ T cells were stimulated with DC pulsed with IgG IC or IHH-IgG IC, as described above, in the presence of 20 U/ml IL-2 for 5 days before purification and i.v. injection of $1x10^6$ T cells into recipient mice having received OVA-B16 cells 24 h earlier. For immunization with *ex vivo* loaded DC, LS-IgG was generated as outlined in Supplementary Experimental Methods and WT DC were loaded for 3 h *ex vivo* with OVA-containing IgG IC or LS-IgG IC and then washed extensively before s.c. footpad injection. For quantification of $CD8^+$ T cells specific for the tumor antigen OVA, lungs were digested with collagenase II as previously described (Olszak et al., 2012) in order to create a single cell suspension. Cells were stained with anti-CD3, anti-CD8 and the SIINFEKL-H2-K^b tetramer or a control LCMV-H2-K^b tetramer (Beckman-Coulter). Frequency of cells positive for the SIINFEKL-H2-K^b tetramer within the $CD3^+CD8^+$ gate was assessed by flow cytometry.

Microbiota Analysis. For T-RFLP analysis, samples were collected from the feces, proximal LI or distal LI of adult (8-week old) and pre-weaning (2-week old) littermates and snap frozen in liquid nitrogen. Samples were processed for T-RFLP analysis as previously described (Uronis et al., 2011). Analysis was conducted using Sequentix Gelquest to assign size (length of fragment) and peak height (abundance) to each TRF. Using PRIMER v6, TRF abundance was standardized by total and transformed by square root. The standardized transformed abundances were compiled into a Bray Curtis similarity matrix and Analysis of Similarity (ANOSIM) was used to test for statistically significant differences in overall community composition between genotypes. Diversity was measured using the Shannon diversity (H),

Margalef richness (d), and Pielou evenness (J) indices and differences were assessed by Student's t test. For qPCR, samples were collected from the feces, proximal LI or distal LI of 7-week old littermates and snap frozen in liquid nitrogen. Samples were processed as described above. qPCR was performed using previously published primer sets (Arthur et al., 2012; Miyamoto et al., 2002; Periasamy and Kolenbrander, 2009; Rabizadeh et al., 2007; Shames et al., 1995).

Flow cytometry. Cells were isolated from the spleen, MLN or colon using collagenase digestion, as previously described (Baker et al., 2011). All antibodies used for flow cytometric staining were purchased from BioLegend except the following: Ki-67 (BD Pharmingen), granzyme B (eBioscience), FCGR4 (Sino Biologicals). Intracellular staining for Granzyme B was carried out using the Cytofix/Cytoperm kit (BD Pharmingen) following a 4 h restimulation by PMA (30 ng/ml) and ionomycin (2 µg/ml) (Sigma) and GolgiStop (BD Pharmingen).

RNA isolation and qPCR. RNA was isolated directly from flow cytometrically sorted cell populations ($CD8^+$ T cells or DC) using an RNeasy MicroKit (Qiagen) or from snap-frozen tissue using an RNeasy MiniKit (Qiagen). RNA was reverse-transcribed using SuperScriptIII (Life Technologies) and quantified by qPCR using SYBR Green technology (Roche).

***In vitro* and *ex vivo* cultures.** $CD8^+$ or $CD4^+$ T cell activation was assessed following 24 h of restimulation with plate-bound anti-CD3 and anti-CD28 using a cytometric bead array (BD Pharmingen). Immune complexes were formed using ovalbumin conjugated to the hapten NIP (4-hydroxy-3-iodo-5-nitrophenylacetic acid) and NIP-specific chimeric IgG (IgG), IHH-IgG or LS-IgG. IHH-IgG is a mutational variant of the chimeric IgG protein which contains a NIP-specific mouse Fab fragment and a human IgG1 Fc fragment and which has been rendered incapable of FcRn binding due to the introduction of mutations in three critical amino acids in the Fc region

which are required for FcRn ligation as previously described (Baker et al., 2011). LS-IgG was generated by introduction of the M428L/N434S mutations which are known to enhance FcRn binding (Zalevsky et al., 2010) into a previously described chimeric antibody specific for the hapten 4-hydroxy-3-iodo-5-nitrophenylacetic acid (NIP) and containing a human IgG1 Fc (Ober et al., 2001) using the QuikChange site-directed mutagenesis kit (Strategene). In vitro cross-presentation assays were carried out by pulsing $1x10^5$ isolated DC with preformed immune complexes (0.5 µg/ml NIP-conjugated OVA + 100 µg/ml anti-NIP IgG or anti-NIP IHH-IgG) for 2-3 h followed by extensive washing and the addition of $2x10^5$ purified OT-I $CD8^+$ T cells (Baker et al., 2011). Cytokine secretion was measured after 24 h or 48 h by ELISA (BD Pharmingen). For IL-12 neutralization experiments, the indicated concentration of IL-12 neutralizing goat IgG (RnD Systems) or goat isotype control IgG (RnD Systems) was added to DC following IgG IC pulsing. DC were incubated in the presence of the neutralizing antibody for 1 h before addition of the OT-I $CD8^+$ T cells.

IgG analysis. IgG isotypes in the serum of untreated or treated mice was quantified using isotype specific ELISAs (Southern Biotech). For quantification of tissue IgG, snap frozen tissue was briefly thawed and then homogenized in PBS containing protease inhibitors (Roche). Insoluble material was removed by centrifugation and protein concentration in the clarified supernatant was assessed by BCA assay (Thermo Scientific). Equivalent quantities of protein were used in IgG isotype ELISAs and IgG concentration was normalized to mg protein. Tumor-specific IgG was evaluated using lysates made from purified tumor epithelial cells, isolated by dispase and collagenase digestion (Baker et al., 2011; Olszak et al., 2012). Tumor lysates were depleted of IgG by overnight incubation with Protein G Sepharose beads (GE Healthcare Life Sciences) at 4°C. For Western blotting, 10 µg lysate from tumor epithelium or normal intestinal epithelium was resolved by SDS-PAGE under reducing conditions and transferred to nitrocellulose membranes. Membrane strips were then probed with 1/10 dilutions of serum or

intestinal homogenates from individual mice and developed with anti-mouse IgG-HRP. Blots were developed with ECL Western Blotting Reagent (GE Healthcare). For ELISA, plates were coated with 1/10 dilution of tumor lysate in coating buffer before application of serial dilutions of serum or tissue homogenates and development with anti-mouse IgG-HRP. OVA-specific IgG-secreting B cells from OVA-B16 metastasis-bearing mice were quantified by ELISpot (MabTech) according to the manufacturer's instructions following isolation of B cells with CD19-microbeads (Miltenyi Biotech).

Nuclear translocation and ChIP. Nuclear tanslocation of transcription factors was assessed following stimulation of isolated DC with IgG IC (formed as above with FcRn-binding IgG or non-FcRn binding IHH-IgG and NIP-OVA) for the indicated times. Nuclei and cytoplasmic fractions were isolated using the NE-PER Nuclear and Cytoplasmic Extraction Kit (Thermo Scientific). Anti-NF-κB p65, anti-IRF-1 and anti-HDAC antibodies were all purchased from Cell Signaling Technologies. ChIP was performed following IC stimulation with the SimpleChIP Plus Enzymatic Chromatin IP Kit (Magnetic Beads) from Cell Signaling Technologies.

Supplemental References

Arthur, J.C., Perez-Chanona, E., Muhlbauer, M., Tomkovich, S., Uronis, J.M., Fan, T.J., Campbell, B.J., Abujamel, T., Dogan, B., Rogers, A.B.*, et al.* (2012). Intestinal inflammation targets cancer-inducing activity of the microbiota. Science *338*, 120-123.

Baker, K., Qiao, S.-W., Kuo, T.T., Aveson, V.G., Platzer, B., Andersen, J.-T., Sandlie, I., Chen, Z., de Haar, C., Lencer, W.I.*, et al.* (2011). Neonatal Fc receptor for IgG (FcRn) regulates cross-presentation of IgG immune complexes by CD8-CD11b+ dendritic cells. Proc. Natl. Acad. Sci. U.S.A. *108*, 9927-9932.

Falo, L.D., Kovacsovics-Bankowski, M., Thompson, K., and Rock, K.L. (1995). Targeting antigen into the phagocytic pathway in vivo induces protective tumour immunity. Nat. Med. *1*, 649-653.

Grivennikov, S.I., Wang, K., Mucida, D., Stewart, C.A., Schnabl, B., Jauch, D., Taniguchi, K., Yu, G.Y., Osterreicher, C.H., Hung, K.E.*, et al.* (2012). Adenoma-linked barrier defects and microbial products drive IL-23/IL-17-mediated tumour growth. Nature *491*, 254-258.

Kruisbeek, A.M. (1991). In Vivo Depletion of CD4- and CD8-Specific T Cells. Curr. Prot. Immunol. *1*, 4.1.1-4.1.5.

LeibundGut-Landmann, S., Osorio, F., Brown, G.D., and Reis e Sousa, C. (2008). Stimulation of dendritic cells via the dectin-1/Syk pathway allows priming of cytotoxic T-cell responses. Blood *112*, 4971-4980.

Miyamoto, Y., Watanabe, K., Tanaka, R., and Itoh, K. (2002). Distribution Analysis of Six Predominant Bacteroides Species in Normal Human Feces Using 16S rDNA-Targeted Species-Specific Primers. Microbial Ecology in Health and Disease *14*, 133-136.

Montoyo, H.P., Vaccaro, C., Hafner, M., Ober, R.J., Mueller, W., and Ward, E.S. (2009). Conditional deletion of the MHC class I-related receptor FcRn reveals the sites of IgG homeostasis in mice. Proc. Natl. Acad. Sci. U.S.A. *106*, 2788-2793.

Ober, R.J., Radu, C.G., Ghetie, V., and Ward, E.S. (2001). Differences in promiscuity for antibody-FcRn interactions across species: implications for therapeutic antibodies. Int. Immunol. *13*, 1551-1559.

Olszak, T., An, D., Zeissig, S., Vera, M.P., Richter, J., Franke, A., Glickman, J.N., Siebert, R., Baron, R.M., Kasper, D.L., and Blumberg, R.S. (2012). Microbial exposure during early life has persistent effects on natural killer T cell function. Science *336*, 489-493.

Periasamy, S., and Kolenbrander, P.E. (2009). Aggregatibacter actinomycetemcomitans Builds Mutualistic Biofilm Communities with Fusobacterium nucleatum and Veillonella Species in Saliva. Infect. Immun. *77*, 3542-3551.

Rabizadeh, S., Rhee, K.-J., Wu, S., Huso, D., Gan, C.M., Golub, J.E., Wu, X., Zhang, M., and Sears, C.L. (2007). Enterotoxigenic Bacteroides fragilis: A potential instigator of colitis. Inflamm. Bowel Dis. *13*, 1475-1483.

Roopenian, D.C., Christianson, G.J., Sproule, T.J., Brown, A.C., Akilesh, S., Jung, N., Petkova, S., Avanessian, L., Choi, E.Y., Shaffer, D.J.*, et al.* (2003). The MHC class I-like IgG receptor

controls perinatal IgG transport, IgG homeostasis, and fate of IgG-Fc-coupled drugs. J. Immunol. *170*, 3528-3533.

Shames, B., Fox, J.G., Dewhirst, F., Yan, L., Shen, Z., and Taylor, N.S. (1995). Identification of widespread Helicobacter hepaticus infection in feces in commercial mouse colonies by culture and PCR assay. J. Clin. Microbiol. *33*, 2968-2972.

Uronis, J.M., Arthur, J.C., Keku, T., Fodor, A., Carroll, I.M., Cruz, M.L., Appleyard, C.B., and Jobin, C. (2011). Gut microbial diversity is reduced by the probiotic VSL#3 and correlates with decreased TNBS-induced colitis. Inflamm. Bowel Dis. *17*, 289-297.

Wirtz, S., Neufert, C., Weigmann, B., and Neurath, M.F. (2007). Chemically induced mouse models of intestinal inflammation. Nat. Protoc. *2*, 541-546.

Yoshida, M., Claypool, S.M., Wagner, J.S., Mizoguchi, E., Mizoguchi, A., Roopenian, D.C., Lencer, W.I., and Blumberg, R.S. (2004). Human neonatal Fc receptor mediates transport of IgG into luminal secretions for delivery of antigens to mucosal dendritic cells. Immunity *20*, 769-783.

Zalevsky, J., Chamberlain, A.K., Horton, H.M., Karki, S., Leung, I.W.L., Sproule, T.J., Lazar, G.A., Roopenian, D.C., and Desjarlais, J.R. (2010). Enhanced antibody half-life improves in vivo activity. Nat. Biotechnol. *28*, 157-159.